New dynamic heat flux sensors to improve energy efficiency of buildings

Bertrand Garnier[a], Ahmed Ould El Moctar[a] , Boussad Azerou[a] and Abdeljahlil Lahmar[b]

[a] Laboratoire de Thermocinétique UMR CNRS6607 Polytech'Nantes, LUNAM, BP50609 44306 Nantes, cedx03,France; bertrand.garnier@univ-nantes.fr, bazerou@mat-ing.com, ahmed.ouldelmoctar@univ-nantes.fr
[b] GEPEA, UMR CNRS6144, LUNAM, IUT 18, Bd Gaston Defferre, 85000 La Roche sur Yon, France; abdeljalil.lahmar@univ-nantes.fr

Abstract:
Heat transfer between building walls and their external surrounding depend on various climatic factors (solar absorption, radiative or convective heat transfer, condensation, evaporation...). To improve energetic performances of buildings, it is important to be able to quantify and follow in time these thermal phenomena. The new dynamic heat flux sensor provides much more information than traditional passive heat flux sensor: one can obtain the evolution of the global heat transfer coefficient and also of the equivalent temperature of the surrounding. In fact the dynamic sensor is equipped with a microheater providing periodically a heat pulse. After each pulse, the temperature relaxation is used to deduce the overall heat transfer coefficient and the equivalent temperature of the surrounding is obtained when the sensor is in equilibrium with the surrounding. In our work, a new design for this sensor is proposed using copper thin films and it is tested for the measurement of the local heat transfer coefficient with an external isothermal flow and compared with theoretical values.

Keywords:
Heat Flux Sensor, Buildings, Thin film, Heat Transfer Coefficient

Nomenclature

C	sensor heat capacity per unit of surface, J/(m^2 K)
h	heat transfer coefficient, W/(m^2 K)
T_a	external temperature, °C
T_c	sensor temperature, °C
T_p	wall temperature, °C
T_E	overall surrounding temperature, °C

Greek symbols

α	wall absorption coefficient
φ	heat flux, W/m^2
τ	time constant, s

Subscripts and superscripts

c	convective
p	wall
r	radiative
s	solar
ν	evaporation

1. Introduction

For energy saving, it is important to improve the thermal management of buildings during their use. For such purpose, it is of great use to follow in real time the heat transfer phenomena outside buildings. However heat transfer between walls and the surrounding depend on many microclimatic factors like wind, rain, infrared or solar radiation... One way is to characterize all the phenomena occurring (convection, radiation, evaporation...). In this case, the resulting wall heat flux φ_p has the following expression:

$$\varphi_p = \varphi_c + \varphi_r + \varphi_v + \alpha_s \varphi_s \quad (1)$$

where :

- the convective heat flux is provided by : $\boldsymbol{\varphi_c = h_c(T_p - T_a)}$ with h_c the convective heat transfer coefficient.
- the infrared radiative heat flux is provided by: $\varphi_r = h_r(T_p - T_r)$ with h_r the radiative heat transfer coefficient depending on wall emissivity, shape factor and on the average temperature T_m where $T_m = (T_p + T_r)/2$
- the heat flux issued from evaporation process: $\varphi_v = h_v(T_p - T_a) + \sigma_v$ where h_v and σ_v are proportional to the latent heat of evaporation.
- the heat flux φ_s from solar radiation is weighted by the wall absorption coefficient α_s

Finally, the overall wall heat flux is provided by:

$$\varphi_p = h_c(T_p - T_a) + h_r(T_p - T_r) + h_v(T_p - T_a) + \sigma_v + \alpha_s\varphi_s \quad (2)$$

The full characterization of all the parameters of eq.(2) would require different types of measurement and is a quite complex work. The alternative which consists in measuring the global heat transfer coefficient and the equivalent surrounding temperature is much more achievable. Indeed, instead of (2) one can write:

$$\varphi_p = h(T_p - T_E) \quad (3)$$

where $h = h_r + h_c + h_v$ is the overall heat transfer coefficient and T_E the overall surrounding temperature given by:

$$T_E = \frac{(h_c + h_v)T_a + h_r T_r - \alpha_s\varphi_s - \sigma_v}{h} \quad (4)$$

To perform the measurements of h and T_E, one needs a specific sensor. Indeed classical heat flux sensor like normal or tangential ones [1,2] can provide the heat flux $\varphi_p(t)$ and wall temperature $T_p(t)$ both versus time but one cannot extract the global heat transfer coefficient h and also the surrounding equivalent temperature T_E. As will be shown later (see section 2), if we use a temperature sensor equipped with a microheater, the sensor being insulated from the wall, it is possible to find the overall heat transfer coefficient h and the surrounding equivalent temperature T_E. Indeed heat pulse is used and the heat transfer coefficient h is extracted during the cooling of the sensor and the equivalent temperature T_E is deduced from the sensor temperature when the heater is turned off. This is repeated every 4 minutes to provide h and T_E values versus time each 4 minutes. This type of sensor was initially proposed by Brunjail [3] in 1982.

In our work, we have designed a new dynamic HFS using thin film heater and resistance thermometer instead of wire heater and thermocouples as proposed by Brunjail [3]. Our new design provides a smaller time constant and a much easier fabrication procedure and will ease the integration of new measurement procedure in the future. In the literature, there is not a lot of work dealing with weather sensors using integrated microheater. So Nguyen [4,5] has designed a thermal sensor to measure continuously the wind velocity and also its angular direction. Its thermal sensor is composed of 40 thermocouples implemented in concentric rings on a disk with a heater on its center. For the same purpose, Ruser [6] has used three resistance temperature detectors (RTD) based on semi conducting materials and the self heating of the RTD crossed with a current of 30 to 80mA.

In this paper, we present first the principle of dynamic heat flux sensor for the estimation of h and T_E and also the two used heat transfer models. Then the new design of this sensor is provided. Finally, it is tested in an isothermal wind tunnel to test its capacity to measure the induced heat transfer coefficient due to the microheating.

2. Working principle of the dynamic heat flux sensor and the used heat transfer models

The sensor has a microheater which can provide heat pulse or constant heat flux (Fig. 1). The sensor temperature T_c is different from T_p and depends on the heat transfer with surrounding and also on the wall temperature *Tp*. The heat flux φ_c through the sensor is:

$$\varphi_c = \varphi_p + \delta\varphi \tag{5}$$

where δφ is the heat flux due to the microheater. One can show that it can be written as [7]:

$$\delta\varphi = h_0(T_c - T_p) \tag{6}$$

If *C* is the heat capacity of the sensor divided by its surface, the balance of energy provides:

$$\varphi_c = h(T_p - T_E) + h_0(T_c - T_p) + C\frac{dT_c}{dt} \tag{7}$$

If the sensor is insulated from the wall as shown on Fig.1 a, we will have through the sensor: $\varphi_p \cong 0$ and then $\varphi_c \cong \delta\varphi$

If $\delta\varphi = 0$ then we have the sensor at T_{c0} and as $\varphi_c = 0$ in eq. (7):

$$0 = h(T_p - T_E) + h_0(T_{c0} - T_p) + C\frac{dT_{c0}}{dt} \tag{8}$$

as $C\, dT_{c0}/dt$ can be neglected:

$$\varphi_p = h(T_p - T_E) \cong h_0(T_p - T_{c0}) \tag{9}$$

Thus instead of finding (h, T_E), one can find (h_0, T_{c0}) the latter being easier to measure.

If $\delta\varphi \neq 0$, one can substract eq (8) to eq.(7) and by using $\theta = T_c(t) - T_{c0}(t)$, we can obtain:

$$\delta\varphi = h\,\theta + C\frac{d\theta}{dt} \tag{10}$$

which solution with $\theta = 0$ for $t = 0$ is:

$$\theta = \frac{\varphi_0}{h_0}\left(1 - exp\left[-\frac{h_0}{C}t\right]\right) \tag{11}$$

if $\delta\varphi = \varphi_0$= constant for t >0. Therefore, the measurement of the time constant τ can provide the heat transfer coefficient h_0 using:

$$\tau = \frac{C}{h_0} \tag{12}$$

Instead of a capacitive model in the HFS sensor, one could have taken into account the conductive heat transfer in its epoxy material. Therefore if we consider an epoxy thermal conductivity λ=0.24 $W.m^{-1}.K^{-1}$ and if we consider the configuration shown in Fig.2, one can have the following expression for the surface temperature of the sensor during its cooling phase [8]:

$$T_c(t) - T_{c0}(t) = \sum_{k=1}^{\infty} A_k\, cos(u_k) e^{-\frac{au_k^2 t}{L^2}}\left(e^{-\frac{au_k^2 t_0}{L^2}} - 1\right) \tag{13}$$

where a is the epoxy thermal diffusivity and the u_k values are provided with the following characteristic equation:

$$u_k \tan(u_k) = \frac{h_0 L}{\lambda} \tag{14}$$

If we measure τ, one can deduce u_1 using $\tau = \frac{L^2}{au_1^2}$ and then h_0 using eq. (14).

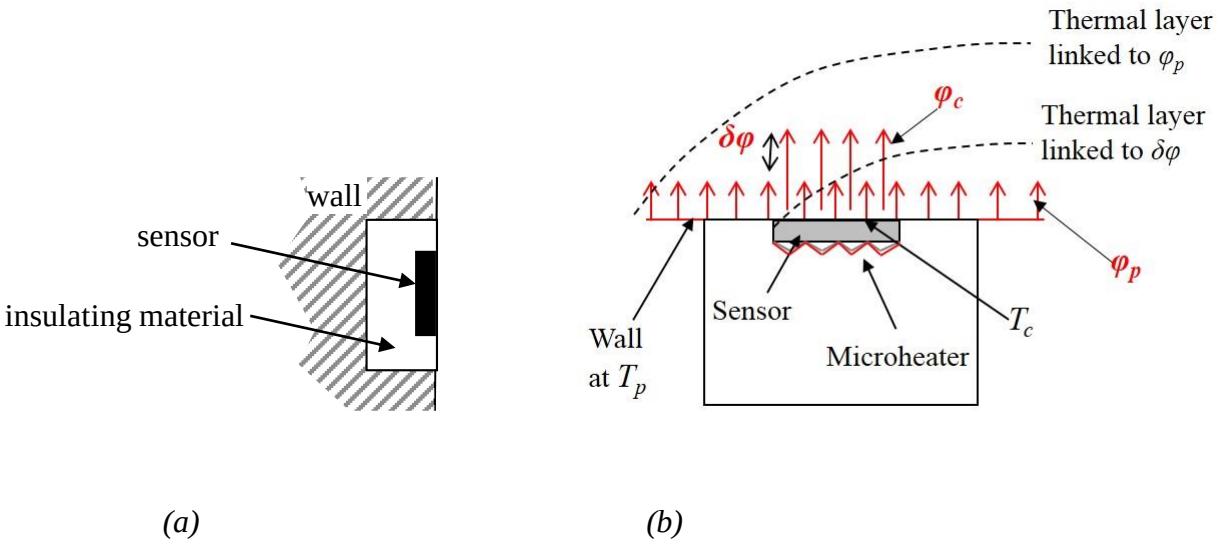

(a) *(b)*

Fig.1. Description of the sensor (a) and perturbation induced by the sensor heater (b)

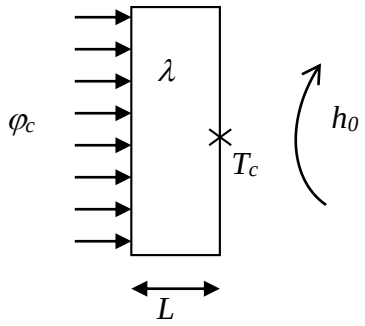

Fig.2. Configuration with a conductive heat transfer model within the heat flux sensor

3. Description of the new dynamic heat flux sensor

As shown on Fig. 3, the new dynamic heat flux sensor was realized with 1.6 mm thick epoxy disk of diameter 60mm with, on both sides, galvanic copper layers 28µm thick. Using masks, copper was removed to have specific patterns for the heater and the resistance temperature detector (RTD). For the heater, the electric pattern covers all the disk and is composed of copper lines with a width of 1 mm while for the temperature measurement the electrical pattern is only on a disk with a diameter 2 times smaller than for the heater. The purpose is to measure the temperature where it is uniform. This was checked with an InSb Flir Titanium infrared camera which has shown that the maximal temperature discrepancy on the sensor pattern is smaller than 0.1°C for the maximal temperature jump of 2.0°C provided by the heating. To protect the copper from oxidation, a tin cold layer was applied on the electric patterns.

For the temperature measurement of the RTD, one has used a Wheatstone bridge which voltage supply was of 44 mV and was computed in order to limit the self heating of the RTD. Indeed, with the 44mV supply voltage, a current of 30mA in the RTD was measured and has induced a maximum temperature jump of only 0.02°C and a parasitic Joule effect of only 0.2 mW. With these operating conditions, the unbalanced voltage of the Wheatstone bridge has shown a sensitivity of 18.7 µV/°C.

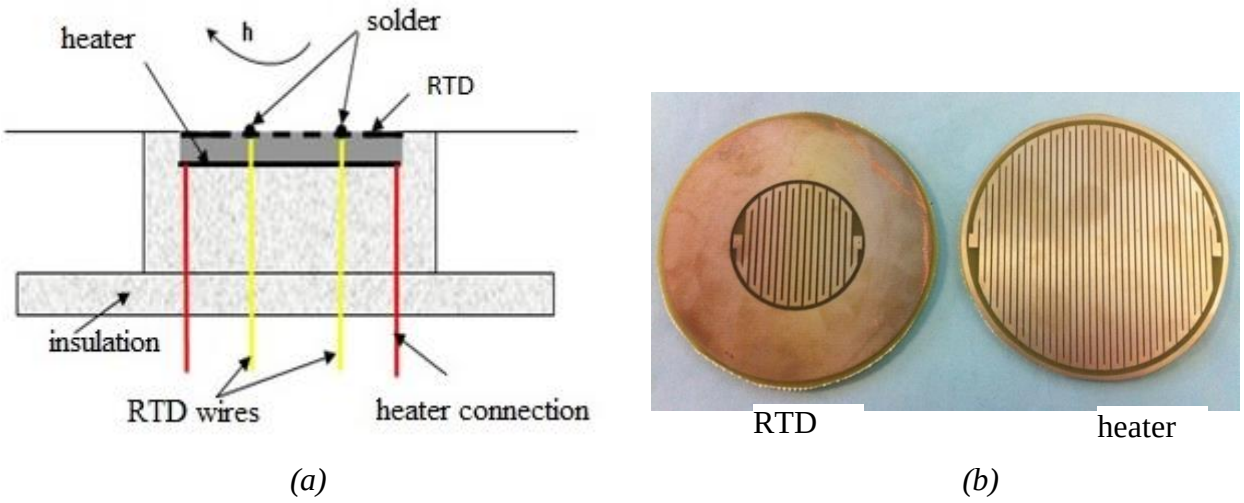

Fig. 3. New dynamic heat flux sensor (a) and temperature sensor (RTD) and heater sides (b)

4. Wind tunnel measurements

The heat flux sensor is implemented in a wood wall which is one of the four wind tunnel test section walls. The sensor is exposed to a laminar air flow. The test section is 1400 mm long and has 300 mm by 300 mm square cross-section (Fig. 4 and 5). The sensor is implemented in the wall with a distance of 600 mm from the wind tunnel inlet.

The air flow is imposed by a fan with varying speed motor. A very laminar flow is obtained thanks to the use of a honeycomb system. A Pitot tube is connected to an electronic micro-manometer (FC 05510 from *Furness Control*) and allows the mean velocity measurement in the external flow (out of the boundary layer).

The studied flow velocity was limited to the range 2 to 12 m/s in order to keep the Reynolds number $Re = \frac{\rho V L_T}{\mu}$ under the value of 5 10^5 corresponding to a laminar boundary layer over a flat plate.

For different flow velocities, the signal of the flux sensor is represented on Fig. 6. This signal corresponds to the temperature measured by the RTD during the heat pulse followed by the cooling period. The same figure shows also the evolution of the prescribed heating voltage with a 4 s duration.

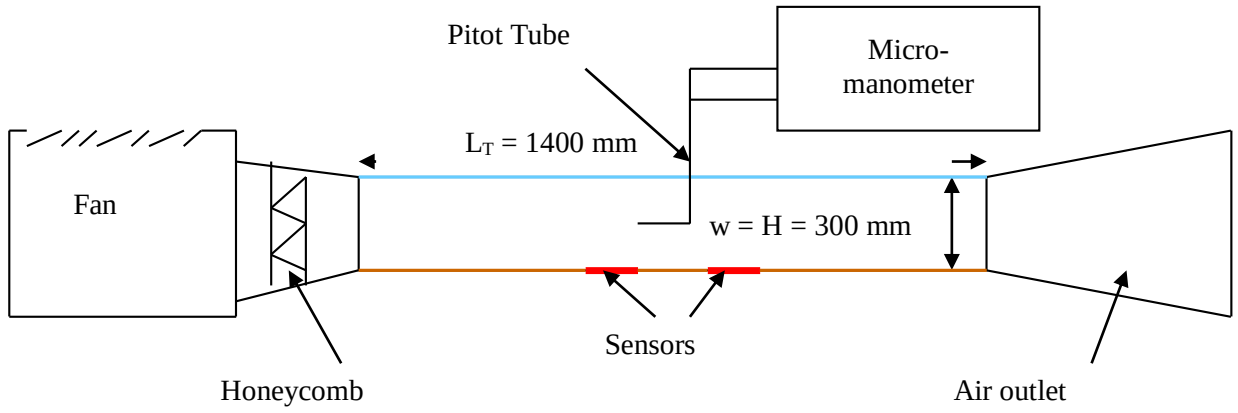

Fig. 4. Wind Tunnel setup.

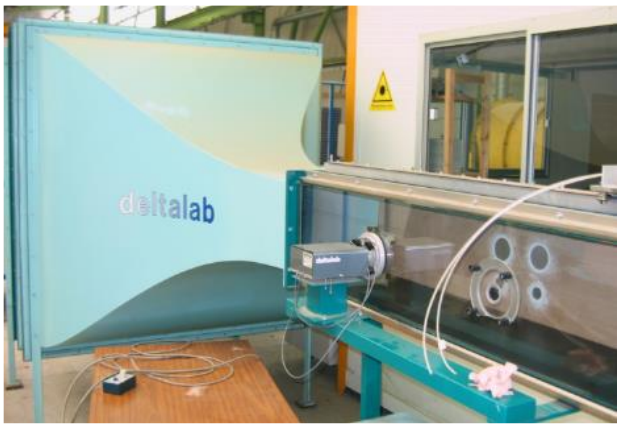

Fig. 5. View of the Wind Tunnel test section with the wall instrumented with flux sensors.

One can observe that except the early part of the beginning of the cooling, the sensor signal presents an exponential relaxation form. We present, on Fig. 7, the evolution of these exponential parts of the signal in terms of $\mathrm{Ln}(T_c - T_c^0)/(T_{max} - T_c^0)$ as function of (t - t_0), with T_{max} the maximum temperature, T_c^0 the sensor temperature without excitation and (t - t_0) the time difference from the initial time corresponding to the beginning of the heating.

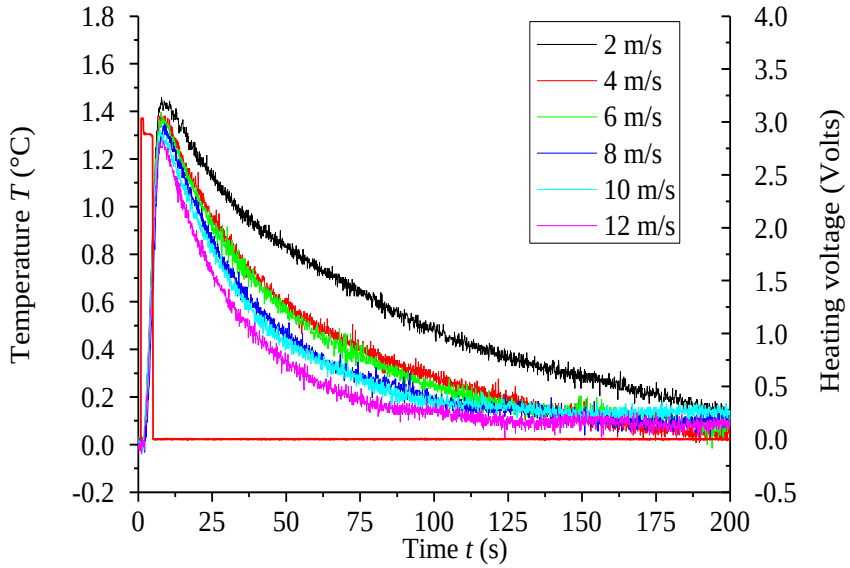

Fig. 6. Temperature time-evolution after a heat pulse..

The linear curves presented on Fig. 7 confirm the exponential behavior of the signal during the cooling period and allow us to infer the coefficient m then the time constant: $\tau = 1/m$. The coefficient m was calculated by linear regression of the signal over the time interval [0s, 75s] where the signal is quite linear.

Then the convective heat coefficient h_0 is deduced by the relationship: $h_0 = -mc = \frac{C}{\tau}$. (eq. 12) for the capacitive model and by using eq.(14) for the conductive model. Considering the geometrical and thermophysical properties of the different elements composing the sensor, we can calculate the sensor capacity which is estimated to be equal to C = 2630 J/(m^{2}K).

For different air speeds, experimental values of τ and h_0 are presented in Table 1 for the capacitive model and in Table 2 for the conductive one. The discrepancies between h_0 values using the two models increases from 3.3% for a 2 m/s velocity to 8.8% for the maximum velocity (12 m/s). As the differences are small, one can use the simplest model that means the capacitive one.

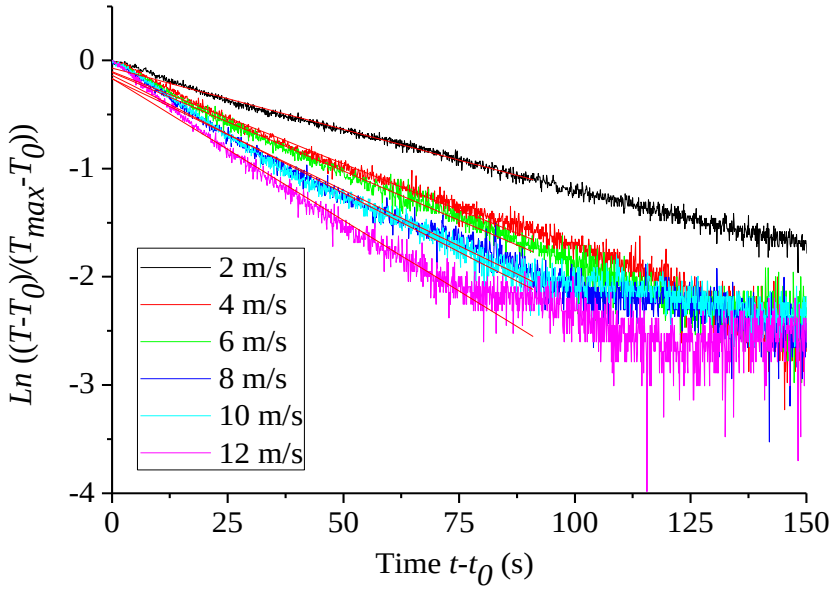

Fig. 7. Log-linear presentation of the exponential cooling signal in the relaxation part.

To analyze the results of Tables 1, we can compare them to Brunjail [3] experimental results and to the theoretical results given by the relationship:

$$Nu = \frac{h.x}{\lambda} = 0.332 Pr^{1/3}.Re^{1/2}\left[1-\left(\frac{x_0}{x}\right)^{3/4}\right]^{-1/3} \quad (15)$$

which is valid in the case of a flat plate with a heating, at constant wall temperature, starting from x_0 [9].

This comparison is presented on Fig. 8. There are some differences between our experimental results and those from Brunjail [3] but also with the theoretical results from eq. (15). It was expected that experimental results show greater values compared to this theoretical relation that is valid in a 2D configuration. Actually in our experimental case, the singularity is more pronounced and that leads to higher value of convective coefficient.

Anyway this was a simple test of the flux sensor in an isothermal flow configuration (the wall where the sensor is set at the same temperature as the air flow). In order to use it in actual configuration we have to test it with a heated wall and to correlate the measured values of this "local" convective coefficient h_0 to the global coefficient over the wall.

Table 1: Experimental values of h_0 with the new dynamic heat flux sensor using eq. (12) corresponding to the capacitive model

Air speed (m/s)	Time constant τ (s)	$h_0 = \frac{C}{\tau}$ (W/(m²K)
2	89.68	29.32 ± 1.08
4	61.84	42.52 ± 1.71
6	60.31	43,6 ± 1.42
8	47.96	54.83 ± 1,87
10	46.68	56.33 ± 2.55
12	36.48	71.48 ± 2.17

Table 2: Experimental values of h_0 with the new dynamic heat flux sensor using eq. (14) corresponding to the conductive model

Air speed (m/s)	Time constant τ (s)	$h_0 = u_1 \frac{\lambda}{L} \tan u_1$ (W/m²K)
2	89.68	30.19 ± 1.7
4	61.84	44.51 ± 2,4
6	60.31	45.70 ± 2.3
8	47.96	58.29 ± 2.96
10	46.68	60.01 ± 3.47
12	36.48	78.38 ± 3.7

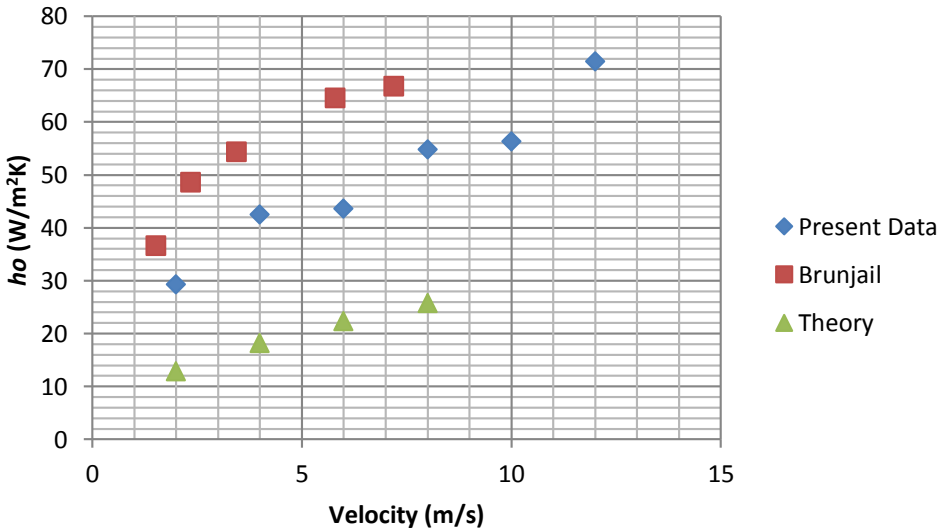

Fig. 8. Comparison of the convective coefficient mean values obtained experimentally in this study with experimental results from Brunjail [3] and theoretical values using eq.(15).

5. Conclusion

The new design heat flux sensor allows the in time survey of various climatic factors such as wind, sun, rain, evaporation.... through the evolution of the overall heat transfer coefficient and equivalent surrounding temperature. Compared to a previous design from Brunjail [3], the use of film for the realization of the heater and the resistance temperature detector induces a 20% smaller time constant.

The flux sensor tests in an isothermal air flow in a laminar wind tunnel has shown the expected behavior of the temperature signal measured by the thermoresistance thin film. Actually, the cooling relaxation part of this signal has an exponential form and leads to the convective coefficient determination through the characteristic time constant. The measured values are less than the ones obtained by Brunjail [3] with a different design of the heat flux sensor. These values are much higher than those given by the theory in 2D flat plate which is due to the 3D localized geometry of our sensor.

This contribution shows the first results dealing with the new designed sensor but additional work is needed to achieve the measurement of the overall heat transfer coefficient h and equivalent surrounding temperature T_E. Ongoing work consists in implementing a heated wall in the wind tunnel to perform non isothermal runs. However one have observed that this sensor is an interesting concept

of heat flux sensor which could be helpful for the thermal management of buildings for energy saving purpose. In addition, the designed sensor has the advantage that it is quite simple and that it will work properly without specific maintenance during its lifetime.

References

[1] Van der Graff, F. 1990, Heat flux sensors, in Ricol, T. and Scholz, J. (eds), Thermal Sensors 4, VCH,Weinheim, Germany-(1990) 297–322.

[2] Khaled M., Garnier B., Harambat F., Peerhossaini H., Heat flux measurements and heat transfer mode analysis in underhood applications, *Measurement Science and Technology* 2010;21 025903

[3] Brunjail C., Fragnaud F., "Capteur à impulsion pour la caractérisation des transferts thermiques entre une paroi et son environnement microclimatique en régime variable", *Revue Phys. Appl.* 1982;17:187-199

[4] Nguyen N.T., "A novel thermal sensor concept for flow direction and flow velocity", *IEEE Sensors Journal* 2005;5:1224-1234

[5] Nguyen N.T., "A novel wind sensor concept based on thermal image measurement using a temperature sensor array", *Sensors and Actuators A* 2004;110:323-327

[6] Ruser H., Horn M., "Low cost weather sensor based on thermal impedance measurements", *Instrumentation and Measurement Technology Conference*-IMTC May 1-3 Warsaw, Poland, 2007.

[7] Fourcher B. Transmission d'un flux thermique sinusoïdal à la frontière de séparation d'un solide et d'un fluide en écoulement permanent, phD University of Nantes 1974.

[8] Carlaw H.S, Jaeger J.C., Heat conduction in solids, 2nd ed., Oxford Science Publication, London 1986.

[9] Kaviany M., Principles of heat transfer, Wiley, New York, 2002.